J Fluoresc (2015) 25:825–834
DOI 10.1007/s10895-015-1543-z

ORIGINAL PAPER

Synthesis, Single X-ray Crystal, Spectroscopic and Photophysical Studies of Novel Heterocyclic Chalcones with Their Biological Application

Salman A. Khan · Abdullah M. Asiri · Hadi Mussa Basisi

Received: 4 December 2014 / Accepted: 23 February 2015 / Published online: 14 April 2015

Abstract Chalcones were synthesized by reaction of 3-acetyl-2,5-dimethylfuran with corresponding active aldehyde in ethanolic NaOH. The structure of these compounds was established by elemental analysis, IR, ^{1}H-NMR, ^{13}C-NMR and EI-MS spectral analysis. UV–vis and fluorescence spectroscopy measurements provided that compounds are good absorbent and fluorescent. Fluorescence polarity study demonstrated that the compounds were sensitive to the polarity of the microenvironment provided by deferent solvents. In addition, spectroscopic and physicochemical parameters, including electronic absorption, extenction coefficient, Stokes shift, oscillator strength and transition dipole moment were investigated in order to explore the analytical potential of synthesized compounds. The anti-bacterial activity of the compounds were first tested in vitro by the disk diffusion assay against two Gram-positive and two Gram-negative bacteria, and then the minimum inhibitory concentration (MIC) was determined with the reference of standard drug Tetracycline. The results showed that compound **3** is better inhibitors of both types of the bacteria (Gram-positive and Gram-negative) as compared to tetracycline.

Keywords Chalcones · Stokes shift · Dipole moment · Anti-bacterial activity · Tetracycline

S. A. Khan (✉) · A. M. Asiri · H. M. Basisi
Chemistry Department, Faculty of Science, King Abdulaziz University, P.O. Box 80203, Jeddah 21589, Saudi Arabia
e-mail: sahmad_phd@yahoo.co.in

A. M. Asiri
Center of Excellence for Advanced Materials Research (CEAMR), King Abdulaziz University, P.O. Box 80203, Jeddah 21589, Saudi Arabia

Introduction

In recent years, organic compounds containing with the donor acceptor framework have attracted a lot of attention because of their potential applications in the fields of material chemistry such as optical communication, optical computing and optical switching [1]. α, β-unsaturated carbonyl compounds (chalcones) containing with the donor group such as NO_2/CN and NR_2/OR are one of best example of the donor acceptor chromophores. Chalcones are well known natural occurring and synthetic compound [2, 3]. It is generally prepared by the reaction of acetophenonne with aromatic aldehydes in the presence of strong base [4]. Chalcones exhibit a wide range spectrum of biological activities such as anti-cancer [5], anti-tumor [6], anti-inflammatory [7], anti-protozoal [8] and anti-viral [9]. α, β-unsaturated carbonyl compounds also form a new and interesting class of compounds that are known to be as effective photosensitive materials [2]. These bichromophoric systems are good models for study of the photoinduced electron transfer process [10]. In addition, chalcones find various applications as photosensitive materials, including second harmonic generation materials in non-linear optics [11], photorefractive polymers [12], holographic recording materials [13] and fluorescent probes for sensing of metal ions [14]. Although the chalcone moiety possesses high photoreactivity [15]. Physicochemical characteristics, such as, solvatochromic, piezochromic, oscillator strength, dipole moment, fluorescent quantum yield and photostability, are also the most important studies for determining the behavior of compounds [16]. In accordance, the present study was aimed to report the synthesis of heterocyclic chalcones and to investigate their in-vitro antibacterial activity. In addition, the analytical efficiency of heterocyclic chalcones was investigated by studying spectroscopic and physicochemical parameters.

Experimental

Chemicals and Reagents

The appropriate 3-acetyl-2,5-dimethylfuran and corresponding active aldehyde were purchased from Acros Organic. Other reagents and solvents (A.R.) were obtained commercially and used without further purification, except dimethylformamide (DMF), ethanol and methanol.

Apparatus

Melting points were recorded on a Thomas Hoover capillary melting apparatus without correction. FT-IR spectra were recorded on a Nicolet Magna 520 FT-IR spectrometer. ^{1}H-NMR and ^{13}C-NMR experiments were performed in $CDCl_3$ on a Brucker DPX 600 MHz spectrometer using tetramethyl silane (TMS) as internal standard at room temperature. UV–vis electronic absorption spectra were acquired on a Shimadzu UV-1650 PC spectrophotometer. Absorption spectra were collected using a 1 cm quartz cell. Steady state fluorescence spectra were measured using Shimadzu RF 5301 PC spectrofluorphotometer with a rectangular quartz cell. Emission spectra were monitored at right angle. All fluorescence spectra were blank subtracted before proceeding in data analyses.

General Method for the Synthesis of Chalcones (1–3)

To a solution of 3-acetyl-2,5-dimethylfuran (0.0025 mol) and corresponding active aldehyde (0.0025 mol) in an ethanolic solution of NaOH (6.0 g, in 10 ml of ethanol) was stirred for 20 h at room temperature. The solution was poured into ice cold water of pH~2 (pH adjusted by HCl). The solid was separated and dissolved in $CHCl_3$, washed with a saturated solution of $NaHCO_3$ and evaporated to dryness. The residue was recrystallized from methanol/ chloroform to give a yellow solid.

(2E)-3-(1-benzyl-1H-indol-3-yl)-1-(2,5-dimethylfuran-3-yl) prop-2-en-1-one (1)

Light-yellow solid: m.p. 102 °C; IR (KBr) ν_{max} cm^{-1}: 3131 (Ar-H), 2917 (C-H), 1644 (C = O), 1556 (C = C); ^{1}H NMR (600MXz, $CDCl_3$) (δ/ppm): 7.77 (d, C = CH, *J*=15.6 Hz,), 7.50 (s, CHaromatic), 7.33- 6.53 (m, 9H CHaromatic), 6.79 (d, CO = CH, *J*=15.6 Hz), 6.37 (s, CHaromatic), 2.35 (s, 2H, −CH_2), 2.25 (s, 3H, −CH_3), 2.21 (s, 3H, −CH_3); ^{13}CNMR ($CDCl_3$) δ: 186.35 (C = O), 157.00, 143.53 (C- β), 137.79, 136.42, 133.42, 132.92, 129.02, 128.16, 127.03, 126.95, 122.95 (C- α), 120.80, 119.85, 113.39, 112.66, 110.69, 110.60, 105.90, 77.06, 76.84, 50.55, 27.30, 14.47; EI-MS *m/z* (rel. int.%) 357 (68) [M+1] $^{+\cdot}$; Anal. calc. for $C_{24}H_{21}NO_2$: C, 81.10, H, 5.96, N, 3.94. Found: C, 81.03, H, 5.92, N, 3.86.

(2E)-1-(2,5-dimethylfuran-3-yl)-3-(1-methyl-1H-pyrrol-2-yl) prop-2-en-1-one (2)

Light-yellow solid: m.p. 106 °C; IR (KBr) ν_{max} cm^{-1}: 3115 (Ar-H), 2944 (C-H), 1644 (C = O), 1562 (C = C); ^{1}H NMR (600MXz, $CDCl_3$) (δ/ppm): 7.71 (d, C = CH, *J*=15.6 Hz,), 7.26 (d, CH aromatic, J = 7.8 Hz), 6.94 (d, CO = CH, *J*= 15.6 Hz), 6.79 (d, CHaromatic, *J*=7.2 Hz), 6.56 (d, CH aromatic, *J*=7.2 Hz), 6.30 (s, 1H, $CHAr_{furane}$), 3.74 (s, 3H, N-CH_3), 2.28 (s, 3H, −CH_3), 2.25 (s, 3H, −CH_3); ^{13}CNMR ($CDCl_3$) δ: 185.64 (C = O), 157.36, 142.85(C- β), 130.31, 130.20, 127.38, 122.72(C- α), 119.19, 111.76, 109.55, 105.69, 34.35, 14.45, 13.29; EI-MS *m/z* (rel. int.%): 231(65) [M+1] $^{+\cdot}$; Anal. calc. for $C_{14}H_{15}NO$: C, 73.34, H, 6.59, N, 6.11. Found: C, 73.28, H, 6.51, N, 6.06.

(2E)-3-(3,5-Dimethyl-1-phenyl-1H-pyrazol-4-yl) -1-(2,5-dimethyl-3-furanyl)prop-2-en-1-one (3)

Light brown; yield: 85 %; m.p. 109–110 °C; IR (KBr) ν_{max}, cm^{-1}: 3043 (C-Haromatic), 2926 (C-Haliphatic), 1636 (C = O), 1562 (C = C); ^{1}H NMR (600 MHz, $CDCl_3$) δ: 7.79 (d, 1H, C7, C = CH, *J*=15.6 Hz,), 6.93 (d, 1H, C8, CO = CH, *J*= 15.6 Hz), 7.27 (s, 1H, C3, $CHAr_{furan}$), 7.49–6.90 (m, 5H, CHaromatic), 2.63 (s, C2, CH_3), 2.51 (s, C5, CH_3), 2.43 (s, C10, CH_3), 2.22 (s, C11, CH_3); ^{13}CNMR ($CDCl_3$) δ: 185.99 (C = O), 157.43, 149.92, 149.21, 141.08(C- β), 138.92, 134.11, 129.24,128.18, 125.17, 124.28, 122.67(C- α), 121.08, 115.25, 114.32, 105.24, 14.51, 14.29, 13.28, 11.60; EI-MS m/z (rel. 135 int.%): 321 (72) [M+1]+; Anal. calc. for $C_{20}H_{20}N_2O_2$: C, 78.98, H, 6.29, N, 8.74; Found: C, 78.93, H, 6.21, N, 8.72.

Materials and Method Crystallography

The sample was examined under microscope and a crystal with 0.42×0.8×0.8 mm size was fixed on glass tip supported by copper magnetic base. The crystal was then mounted on Agilent SuperNova (Dual source) Agilent Technologies Diffractometer, equipped with graphite-monochromatic Cu/ Mo Kα radiation for data collection. Data reduction was carried out using CrysAlisPro software [17] at 296 K under the Cu Kα radiation. The structure solution and refinement was performed using SHELXS–97 [18], in-built with X-Seed [19]. All non–hydrogen atoms were refined anisotropically by full–matrix least squares methods [20].

All C-H atoms were positioned geometrically and treated as riding atoms with $C_{aromatic}$–H=0.93, C_{methyl}–H=0.96 and Uiso(H)=1.2 Ueq (C) for aromatic carbon atoms while Uiso(H)=1.5 Ueq(C) for methyl carbon atoms. The figures

Scheme 1 Synthetic route of compound 1–3

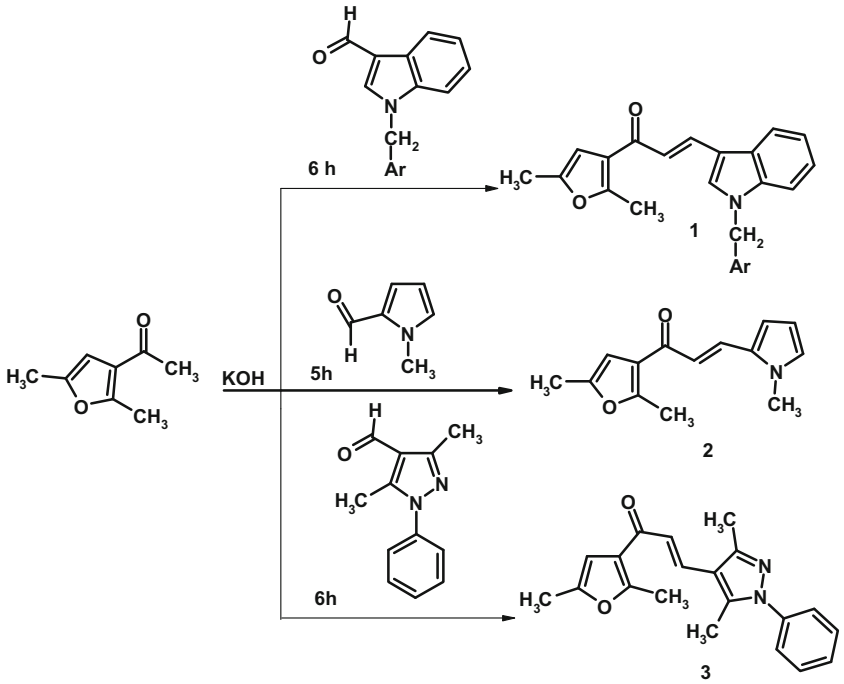

were drawn using Mercury [21], *ORTEP-3* [22] and PLATON [23] programs in built with Wingx [24, 25]. The Data has been submitted to CCDC with CCDC code 1031075 and it can be obtained freely from http://www.ccdc.cam.ac.uk/Community/Requestastructure/Pages/DataRequest.aspx.

Organism Culture and In Vitro Screening

Anti-bacterial activity was studied by the disk diffusion method with minor modifications. *A. hydrophila, Y.enterocolitica, L. Monocytogenes and P. aeruginosa* were subcultured in BHI medium and incubated for 18 h at 37 °C. The bacterial cells were then suspended, according to the McFarland protocol, in saline solution to produce a suspension of about 10^{-5} CFU mL^{-1}. An amoun of 10 μL of this suspension was mixed with 10 mL of sterile antibiotic agar at 40 °C and poured onto an agar plate in a laminar flow cabinet. Five paper disks (6.0 mm diameter) were fixed onto the nutrient agar plate. 1 mg of each tested compound was dissolved in 100 μL DMSO to prepare standard solutions of 10, 20, 25, 50 and 100 μg/μL. All solutions were individually poured onto each disk plate. Tetracycline (30 μg/disk) was used as standard drug (positive control). A DMSO poured disk was used as negative control. The susceptibility of the bacteria to tested compounds was

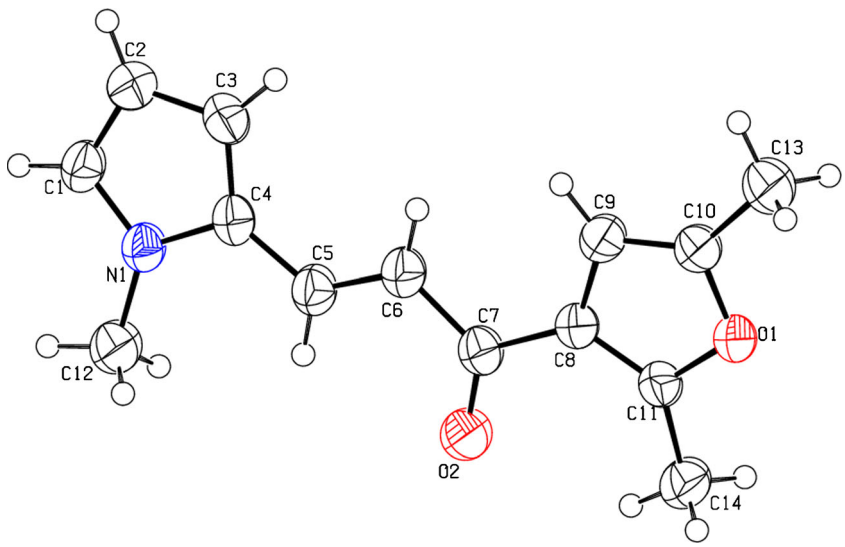

Fig. 1 ORTEP diagram of 1, thermal ellipsoids were drawn at 50 % probability level

Table 1 Crystal data and structure refinement for 1

Identification code	14042
Empirical formula	$C_{14}H_{15}NO_2$
Formula weight	229.27
Temperature/K	296.15
Crystal system	tetragonal
Space group	$I4_1/a$
a/Å	19.0942(4)
b/Å	19.0942(4)
c/Å	13.7323(3)
α/°	90.00
β/°	90.00
γ/°	90.00
Volume/Å^3	5006.64(18)
Z	16
ρ_{calc}mg/mm^3	1.217
m/mm^{-1}	0.655
F(000)	1952.0
Crystal size/mm^3	0.42×0.08×0.08
2Θ range for data collection	7.94 to 152.56°
Index ranges	−20≤h≤24, −16≤k≤22, −17≤l≤11
Reflections collected	7859
Independent reflections	2608[R(int) = 0.0225]
Data/restraints/parameters	2608/0/157
Goodness-of-fit on F^2	1.087
Final R indexes [I>=2σ (I)]	R_1=0.0435, wR_2=0.1207
Final R indexes [all data]	R_1=0.0551, wR_2=0.1294
Largest diff. peak/hole / e Å^{-3}	0.20/−0.17

determined by the formation of an inhibitory zone after 18 h of incubation at 36 °C. Table 8 reports the inhibition zones (mm) of each compound and the control. The minimum inhibitory concentration (MIC) was evaluated by the macro dilution test using standard inoculums of 10^{-5} CFL mL^{-1}. Serial dilutions of tested compounds, previously dissolved in dimethyl sulfoxide (DMSO), were prepared to final concentrations of 512, 256, 128, 64, 32, 16, 8, 4, 2 and 1 μg/mL. A volume of 100 μL

Table 2 Bond lengths for 14042

Atom	Atom	Length/Å	Atom	Atom	Length/Å
O1	C10	1.3794(18)	C4	C5	1.435(2)
O1	C11	1.3638(17)	C5	C6	1.338(2)
O2	C7	1.2313(18)	C6	C7	1.469(2)
N1	C1	1.3546(19)	C7	C8	1.4737(18)
N1	C4	1.3861(17)	C8	C9	1.429(2)
N1	C12	1.452(2)	C8	C11	1.362(2)
C1	C2	1.362(2)	C9	C10	1.335(2)
C2	C3	1.398(2)	C10	C13	1.488(2)
C3	C4	1.383(2)	C11	C14	1.474(2)

Table 3 Bond angles for 14042

Atom	Atom	Atom	Angle/°	Atom	Atom	Atom	Angle/°
C11	O1	C10	107.44(11)	O2	C7	C8	120.82(13)
C1	N1	C4	109.04(13)	C6	C7	C8	117.73(13)
C1	N1	C12	124.18(13)	C9	C8	C7	128.51(13)
C4	N1	C12	126.77(13)	C11	C8	C7	125.23(13)
N1	C1	C2	108.99(13)	C11	C8	C9	106.26(12)
C1	C2	C3	107.36(14)	C10	C9	C8	107.47(13)
C4	C3	C2	108.02(13)	O1	C10	C13	115.86(14)
N1	C4	C5	121.78(13)	C9	C10	O1	109.44(13)
C3	C4	N1	106.58(13)	C9	C10	C13	134.70(16)
C3	C4	C5	131.59(13)	O1	C11	C14	115.93(13)
C6	C5	C4	127.13(15)	C8	C11	O1	109.39(12)
C5	C6	C7	120.91(15)	C8	C11	C14	134.68(14)
O2	C7	C6	121.44(13)				

was added to each tube of a 24 h old inoculum. The MIC, defined as the lowest concentration of the tested compound which inhibits the visible growth after 18 h, was determined visually after incubation for 18 h at 37 °C, the results are presented in Table 9. Tests using DMSO and tetracycline as negative and positive controls were also performed.

Results and Discussion

Synthesis and Characterization

Chalcones were synthesized by the reaction of 3-acetyl-2,5-dimethylfuran and corresponding active aldehyde (Scheme 1) [26]. The purified products was characterized by the EI-MS m/z (rel. int.%): FT-IR, ^{1}H-NMR, ^{13}C-NMR and elemental analysis. The IR spectra of chalcones show the characteristic band. The ν(C = O) peak of Act-furan observed at 1668 cm^{-1} shifts to a lower frequency of 1636–1644 cm^{-1} of chaconnes. This is due to the conjugation of the π-electrons on the benzene moiety with those on the ethylene moiety in the enon linkage. ^{1}H-NMR spectra, which prove diagnostic tool for the positional elucidation of the proton. Assignments of the signals are based on chemical shift and intensity pattern. The ^{1}H-NMR spectra of all the compounds (1–3) measured at room temperature shows two doublets at 7.71−7.79 ppm (J=15.6) for the CH = C and 6.79–6.94 ppm (J=15.6 Hz) for the CO = CH indicating that the ethylene moiety in the enon linkage is in the *trans*-conformation which conform the formation of the chalcones (1–3). The appearance of multiplets at δ 7.33−6.30 was due to aromatic protons. ^{13}C NMR ($CDCl_3$) spectra of chalcones (1–3) were recorded in $CDCl_3$ and spectral signals are in good agreement with the probable structures. ^{13}C-NMR spectra showed

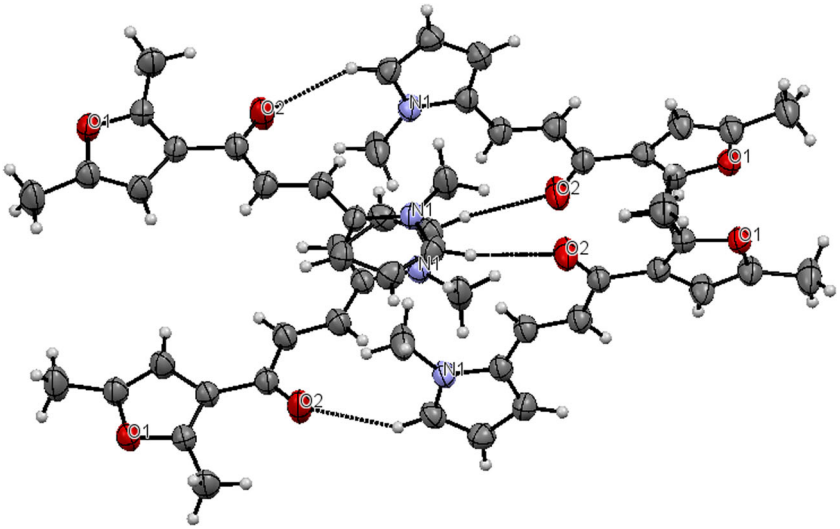

Fig. 2 A view showing the hydrogen bonding interaction which connects four molecules

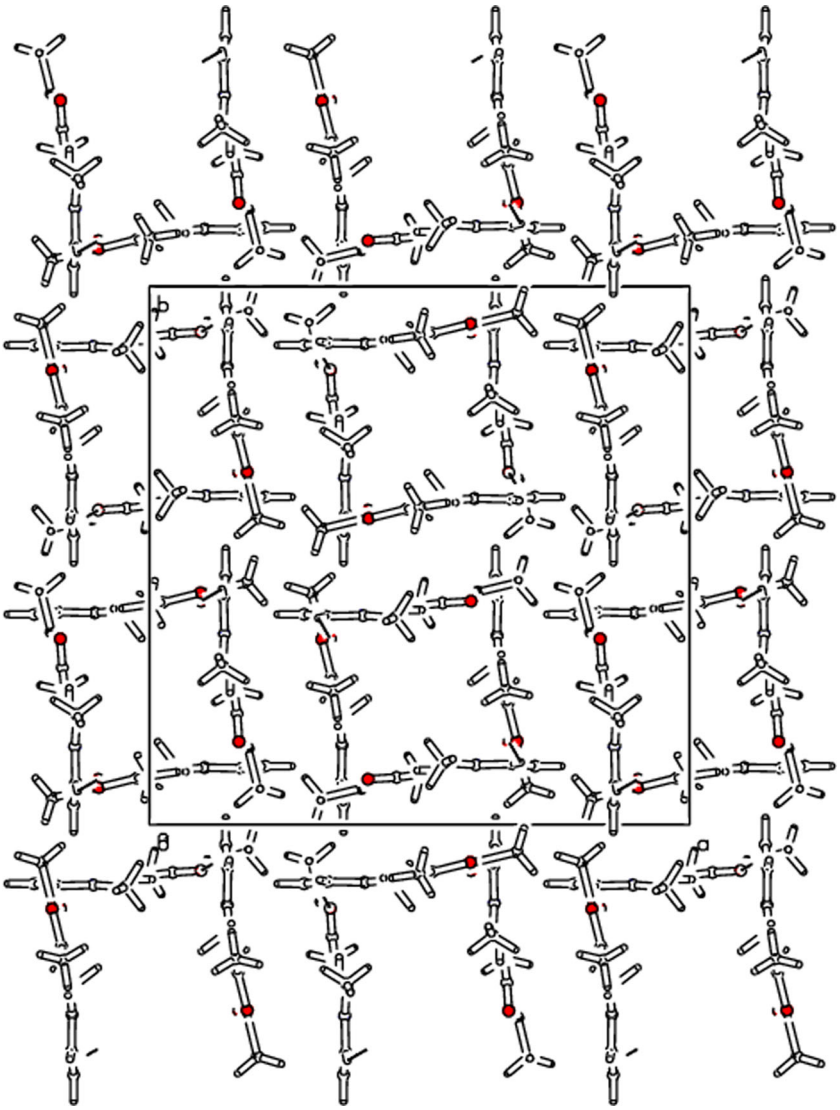

Fig. 3 A unit cell packing view showing the formation of squares through the interaction of molecules

Table 4 Hydrogen bonds for 14042

D	H	A	d(D-H)/Å	d(H-A)/Å	d(D-A)/Å	D-H-A/°
C1	H1	O2[1]	0.93	2.44	3.2703(18)	148.4

[1] 5/4-Y,1/4+X,5/4-Z

signals at 141.08−143.53 and 122.67−122.95 ppm due to (C-β) and (C- α) which is conformed the formation of chalcones. Details of ^{13}C-NMR spectra of compounds were given in the experimental section. Finally characteristic peaks were observed in the mass spectra of the compounds (1–3) by the molecular ion peak. The mass spectrum of compound 1 shows a molecular ion peak ($M^{+\cdot}$) m/z 357. All the compounds give similar fragmentation pattern.

Single X-ray Crystal

In order to understand the structural interactions between the molecules in a unit cell and their spatial arrangements we crystalized compound 2 and diffracted at room temperature. *ORTEP* diagram is presented in Fig. 1, crystallographic data and unit cell dimensions are given in Table 1. Selected bond length and bond angle are shown in Tables 2 and 3. The molecule was crystalized in trigonal crystal system with space group I 41/a. In the molecule the pyrole (C1-C4/N1) and furan (C8-C11/O1) rings are connected through the backbone consisting of three carbon atoms. Both the rings are twisted at dihedral angle of 14.28 (4)°. The molecule afforded weak C-H…O type hydrogen bonding interaction Figs. 2 and 3, Table 4 and connects the four molecules to generate a square shape. Solvent volume per unit cell was determined using SQUEEZE option of PLATON which is 57.00 Å^3(1.14 % of the cell volume).

Spectral Behaviour of Chalcones in Different Media

Absorption and emission spectra of 1×10^{-5} mol dm^{-3} compounds (1–3) in various non-polar, polar aprotic and protic solvents were studied (Figs. 4a, 5 and 6b). Calculated physicochemical parameters obtained from steady state absorption

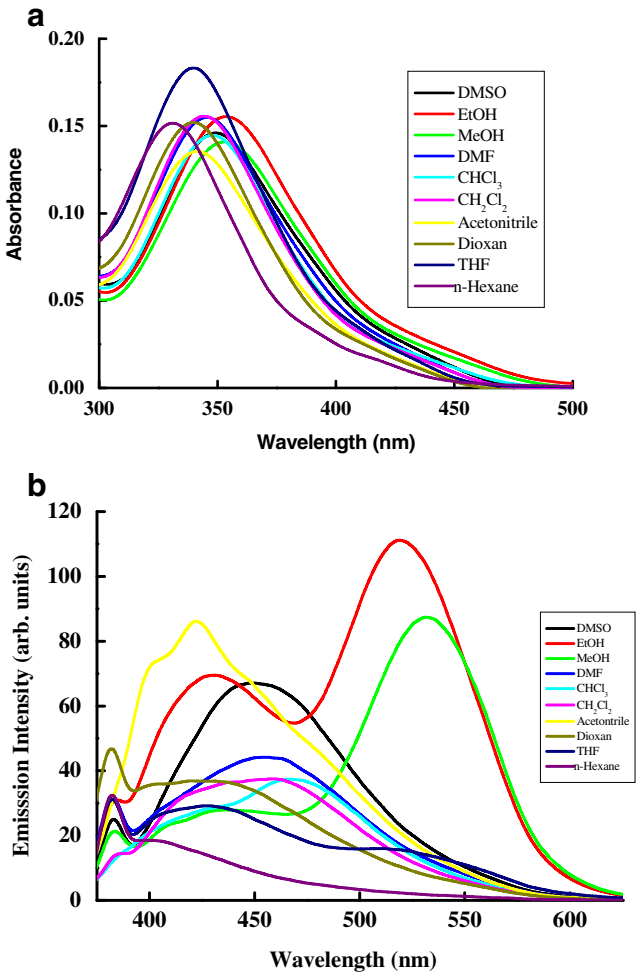

Fig. 4 **a**. Electronic absorption spectra of 1×10^{-5} mol dm^{-3} of compound **1** in different solvents. **b**. Emission spectra of 1×10^{-5} mol dm^{-3} of compound **1** in different solvents

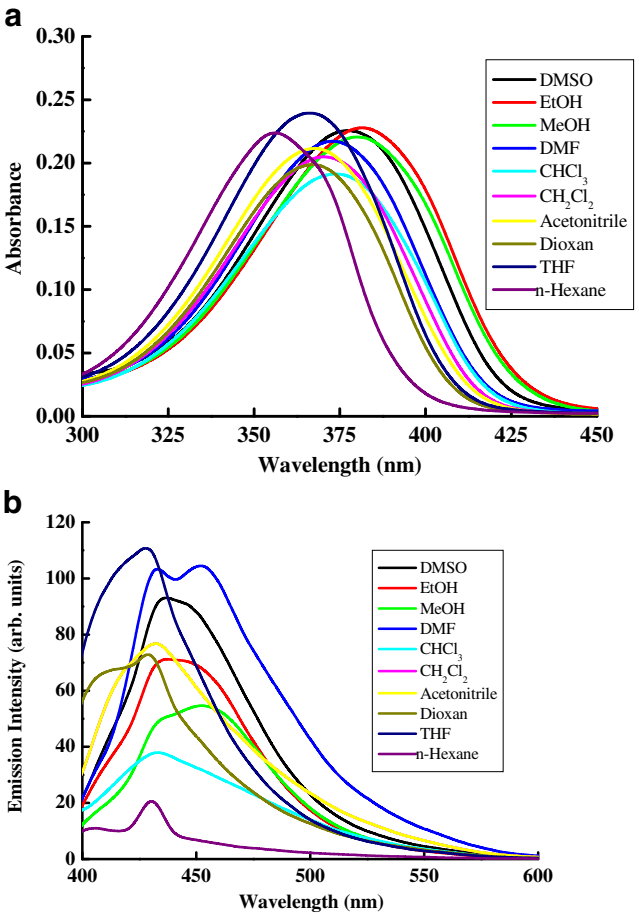

Fig. 5 **a** Electronic absorption spectra of 1×10^{-5} mol dm^{-3} of compound **2** in different solvents. **b**. Emission spectra of 1×10^{-5} mol dm^{-3} of compound **2** in different solvents

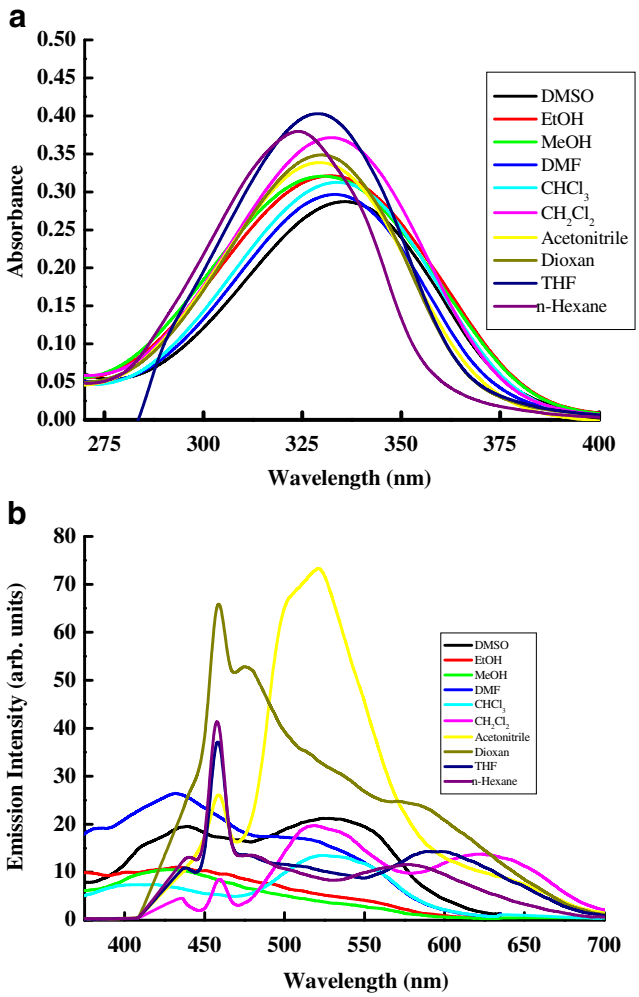

Fig. 6 **a** Electronic absorption spectra of 1×10^{-5} mol dm^{-3} of compound **3** in different solvents. **b**. Emission spectra of 1×10^{-5} mol dm^{-3} of compound **3** in different solvents

and fluorescence spectra of compounds (1–3) were measured and listed in Tables 5, 6 and 7. A close examination of Figs. 4a, 5 and 6a displays that the polarity of solvent has a little effect on absorption maxima, indicating the weak polar character of compounds (1–3) in the ground state. However, the emission spectra of these compounds are broad and red shifted as the solvent polarity increases, as shown in Figs. 4b, 5 and 6b. The red-shift in n-Hexane to DMSO indicates that photoinduced intramolecular charge transfer (ICT) occurring in the singlet excited state from electron donating group to electron acceptor group [27]. As a result, the polarity of compounds (1–3) increases on excitation.

Determination of Oscillator Strength and Transition Dipole Moment

The solvatochromic behavior in compounds (1–3) allows one to determine the difference in the dipole moment between the excited singlet and the ground state ($\Delta\mu=\mu_e-\mu_g$). This difference can be obtained using the simplified Lippert- Mataga equation as follows [27, 28]:

$$\Delta\overline{\nu}_{st}=\frac{2\left(\mu_e-\mu_g\right)^2}{hca^3}\Delta f+Const. \quad (1)$$

$$\Delta f=\frac{D-1}{2D+1}-\frac{n^2-1}{2n^2+1} \quad (2)$$

where $\Delta\overline{\nu}_{st}$ is the Stokes–shift [29], which increases with increasing the solvent polarity pointing to stronger stabilization of the excited state in polar solvents, h denotes Planck's constant, c refers to the speed of light in vacuum and a is the Onsager cavity radius. Parameters D and n, in Eq. (2), correspond to the dielectric constant and refractive index of the solvent, respectively. The Onsager cavity radius was chosen to be 4.2 Å because this value is comparable to the radius of a typical aromatic fluorophore [30]. Stokes shifts ($\Delta\overline{\nu}_{ss}$) of compounds (1–3) in different solvents were calculated, as

Table 5 Spectral data of compound no. **1** in different solvents

Solvent	Δf	E_T^N	E_T (30) Kcal mol^{-1}	λ_{ab}(nm)	λ_{em}(nm)	ε M^{-1} cm^{-1}	f	μ_{12} Debye	$\Delta\overline{\nu}$ (cm^{-1})
DMSO	0.266	1.52	80.08	357	448	14,700	0.33	5.29	5690
EtOH	0.305	1.49	78.98	362	518	15,600	0.51	6.63	8319
MeOH	0.308	1.49	79.19	361	531	14,200	0.50	6.55	8868
DMF	0.263	1.54	80.76	354	445	15,600	0.36	5.50	5777
$CHCl_3$	0.217	1.54	80.53	355	458	14,600	0.36	5.51	6335
CH_2Cl_2	0.255	1.55	81.22	352	446	15,700	0.37	5.56	5988
Acetonitrile	0.274	1.57	81.68	350	422	13,700	0.26	4.65	4875
Dioxan	0.148	1.59	82.39	347	419	15,400	0.30	4.97	4952
THF	0.208	1.60	82.63	346	419	18,600	0.37	5.52	5035
n-Hexane	0.0014	1.66	84.58	338	392	31,700	0.25	4.48	4075

Table 6 Spectral data of compound no. **2** in different solvents

Solvent	Δf	E_T^N	E_T (30) Kcal mol^{-1}	λ_{ab}(nm)	λ_{em}(nm)	ε M^{-1} cm^{-1}	f	μ_{12} Debye	$\Delta\overline{\nu}$ (cm^{-1})
DMSO	0.266	1.34	74.26	385	441	22,600	0.29	5.15	3299
EtOH	0.305	1.32	73.49	389	449	22,900	0.31	5.35	3435
MeOH	0.308	1.32	73.68	388	457	22,100	0.34	5.60	3892
DMF	0.263	1.38	75.43	379	445	21,900	0.34	5.53	3914
$CHCl_3$	0.217	1.36	75.04	381	439	20,600	0.26	4.85	3467
CH_2Cl_2	0.255	1.38	75.63	378	437	20,600	0.29	5.10	3572
Acetonitrile	0.274	1.39	76.03	376	435	21,250	0.30	5.18	3607
Dioxan	0.148	1.40	76.24	375	435	20,000	0.29	5.08	3893
THF	0.208	1.42	76.85	372	435	24,100	0.37	5.72	3893
n-Hexane	0.0014	1.48	78.76	363	435	22,800	0.41	5.95	4560

shown in Tables 5, 6 and 7, using the following the equation [27]

$$\Delta\overline{\nu}_{ss} = \overline{\nu}_{ab} - \overline{\nu}_{em} \tag{3}$$

where $\overline{\nu}_{ab}$ and $\overline{\nu}_{em}$ denote the wavenumbers of excitation and emission maxima (cm^{-1}), respectively. The change in dipole moments ($\Delta\mu$) between the excited singlet and ground state were calculated as 9.19, −4.72 and −1.54 Debye for compounds (1–3). Positive value for compound 1 indicating that the excited sate is more polor than the ground state and negative value for compound 2 & 3 indicating that the ground sate is more polor than the excited state.

The effective number of electrons transition from the ground to excited state is usually described by the oscillator strength, which provides the absorption area in the electronic spectrum. The oscillator strength, *f*, can be calculated using the following equation [31]:

$$f = 4.32 \times 10^{-9} \int \varepsilon(\overline{\nu})\, d\overline{\nu} \tag{4}$$

where ε is the extinction coefficient ($Lmol^{-1}$ cm^{-1}), and $\overline{\nu}$ represents the numerical value of wavenumber (cm^{-1}). Oscillator strength values of compounds (1–3) in different solvents are reported in Tables 1, 2 and 3. In addition, the transition dipole moment (μ) for compounds **1**–**3** from ground to excited state in Debye was estimated in different solvents (Tables 1, 2 and 3) using the following relation [32]

$$\mu^2 = \frac{f}{4.72 \times 10^{-7} \times E_{max}} \tag{5}$$

where E_{max} is the maximum energy of absorption in cm^{-1}

Fluorescence Polarity Study of Chalcones 1–3

The steady state absorption and fluorescence parameters of 1×10^{-5} M were recorded in various polar aportic and polar protic solvents, as summarized in Table 1, 2 and 3. The emission spectra of compounds 1–3 are shown in Figs. 1b, 2 and 3b. It can be clearly noted from Figs. 1b, 2 and 3b that the polarity of solvent has a significant effect on emission spectra,

Table 7 Spectral data of compound no. **3** in different solvents

Solvent	Δf	E_T^N	E_T (30) Kcal mol^{-1}	λ_{ab}(nm)	λ_{em}(nm)	ε M^{-1} cm^{-1}	f	μ_{12} Debye	$\Delta\overline{\nu}$ (cm^{-1})
DMSO	0.266	1.64	83.84	341	513	28,700	1.12	9.53	9832
EtOH	0.305	1.67	85.09	336	439	32,100	0.89	8.46	6982
MeOH	0.308	1.67	85.09	336	426	32,000	0.80	8.00	6287
DMF	0.263	1.66	84.58	338	439	29,700	0.80	8.02	6806
$CHCl_3$	0.217	1.66	84.58	338	515	31,300	1.27	10.10	6806
CH_2Cl_2	0.255	1.66	84.83	337	592	37,100	1.59	11.29	10,770
Acetonitrile	0.274	1.69	85.60	334	527	33,900	1.48	10.29	10,965
Dioxan	0.148	1.68	85.34	335	475	34,800	1.23	9.90	8888
THF	0.208	1.69	85.60	334	462	40,200	1.33	10.28	8295
n-Hexane	0.0014	1.73	86.90	329	444	38,000	1.19	9.65	7873

Table 8 Antibacterial activity of chalcones (1–3) positive control: Tetracycline and negative control (DMSO) measured by the Halo Zone Test (Unit, mm)

Compounds	Corresponding effect on microorganisms			
	A.hydrophila	*Y.enterocolitica*	*L.monocytogenes*	*P.aeruginosa*
1	11.5±0.5	12.4±0.5	9.8±0.2	10.4±0.5
2	10.4±0.3	11.2±0.3	9.0±0.4	10.5±0.2
3	15.8±0.5	22.5±0.5	18.2±0.5	17.5±0.5
Tetracycline	13.0±0.5	20.0±0.5	12.0±0.5	14.0±0.5
DMSO	–	–	–	–

indicating the strong polar character of all compounds in the ground state. The emission spectra, however, are broad and red shifted as the solvent polarity increases from n-hexane to DMSO. Compounds 3 gives two bands Fig. 3b that is locally excited state (LE) associated with interamolecular charge transfer (ICT) of the compound because of the donor group N and acceptor group C = O is presence in the compound 3. The empirical Dimroth polarity parameter, $E_T(30)$ and E^NT of compound (1-3), was also calculated according to the following equation [33].

$$E_T^N = \frac{E_T(solvent) - 30.7}{32.4} \tag{6}$$

$$E_T(solvent) = \frac{28591}{\lambda_{max}} \tag{7}$$

where λ_{max} corresponds to the peak wavelength (nm) in the red region of the intramolecular charge transfer absorption of all compounds. The red (bathochromic) shift from n-hexane to DMSO indicates that photoinduced intramolecular charge transfer (ICT) occurs in the singlet excited state, and the polarity of compounds, therefore, increases on excitation.

Antimicrobial Activity: Disc–Diffusion and Micro Dilution Assay

All the compounds were tested for their antibacterial activities by disc-diffusion method using nutrient broth medium [contained (g/L): beef extract 3 g; peptone 5 g; pH 7.0 [34]. The Gram-positive bacteria and Gram-negative bacteria utilized in this study consisted of *A. hydrophila, Y. enterocolitica, L. monocytogenes and P. aeruginosa*. In the disc-diffusion method, sterile paper discs (0.5 mm) impregnated with compound, dissolved in dimethylsulfoxide (DMSO) at concentration 100 μg/mL, were used. The paper discs impregnated with the solution of the tested compound were then placed on the surface of the media inoculated with the microorganism. The plates were incubated at 35 °C for 24 h, the growth inhibition zones are shown in Table 8. Chalcone derivatives were further checked by MIC method, as illustrated in Table 9.

Conclusion

A chalcone was prepared by the reaction of 3-acetyl-2,5-dimethylfuran with corresponding active aldehyde in ethanolic NaOH. Physicochemical studies of the compounds including singlet absorption, extinction coefficient, Stokes shift, oscillator strength, dipole moment, were investigated on the basis of the polarity of solvent. The absorption spectra of chalcones exhibit an intramolecular charge transfer band; which showed a positive solavotochromism in different solvents. The emission spectra of the dyes also reveal the intramolecular charge transfer band character. These findings confirm that there is a significant electron transfer between the donating moiety and the accepting fragment through the π conjugated. The antibacterial activity of the chalcones was examined using culture of bacteria and the results showed that the nitrogen containing chalcone showed good the

Table 9 Minimum inhibition concentration (MIC) of chalcones (1–3), positive control: Tetracycline

Compounds	Corresponding effect on microorganisms			
	A.hydrophila	*Y.enterocolitica*	*L.monocytogenes*	*P.aeruginosa*
1	128	128	128	64
2	64	64	128	128
3	32	32	16	32
Tetracycline	32	32	32	32
DMSO	–	–	–	–

antibacterial activity. Among the entire three compounds, pyrazol containing of chalcone **(3)** showed better antibacterial activity than the reference drug tetracycline.

Acknowledgments This Project was funded by the King Abdulaziz City for Science and Technology (KACST) through National Science, Technology and Innovation Plan (NSTIP) under grant number 8-ENE198-3. The authors, therefore, acknowledge with thanks KACST for support for Scientific Research. Also, the authors are thankful to the Deanship of Scientific Research (DSR), King Abdulaziz University for their technical support.

References

1. Asiri AM, Khan SA, Al-Amodi MS, Alamry KA (2012) Synthesis, characterization absorbance, fluorescence and non linear optical properties of some donor acceptor chromophores. Bull Kor Chem Soc 33:1900–1906
2. Marwani HM, Asiri AM, Khan SA (2013) Spectral, stoichiometric ratio, physicochemical, polarity and photostability studies of newly synthesized chalcone dye in organized media. J Lumin 136:296–302
3. Asiri AM, Khan SA, Hallag SI (2011) Electrochemical studies of some carbazole derivatives via cyclic voltammetry and convolution - deconvolution transforms. J New Mater Electrochem Syst 14:251–258
4. Asiri AM, Khan SA (2011) Synthesis, characterization and optical properties of mono- and bis-chalcone. Mater Lett 65:1749
5. Mai CM, Yaeghoobi M, Abd-Rahman N, Kang YB, Pichika MR (2014) Chalcones with electron-withdrawing and electron-donating substituents: anticancer activity against TRAIL resistant cancer cells, structure–activity relationship analysis and regulation of apoptotic proteins. Eur J Med Chem 77:378–387
6. Bandgar BP, Gawande SS, Bodade RG, Totre JV, Khobragade CN (2010) Synthesis and biological evaluation of simple methoxylated chalcones as anticancer, −anti-inflammatory and antioxidant agents. Bioorg Med Chem 18:1364–1370
7. Cheng J, Hung C, Yang S, Wang J, Won S, Lin C (2008) Synthesis and cytotoxic, anti-inflammatory, and anti-oxidant activities of 2′,5′-dialkoxylchalcones as cancer chemopreventive agents. Bioorg Med Chem 16:7270–7276
8. Parveen H, Hayat F, Salahuddin A, Azam A (2010) Synthesis, characterization and biological evaluation of novel 6-ferrocenyl-4-aryl-2-substituted pyrimidine derivatives. Eur J Med Chem 45:3497–3503
9. Asiri AM, Khan SA (2012) Synthesis, characterization, and in vitro antibacterial activities of macromolecules derived from bis-chalcon. J Heterocycl Chem 49:1434–1438
10. Yesuthangam Y, Pandian S, Venkatesan K, Gandhidasan R, Murugesan R (2011) Photogeneration of reactive oxygen species and photoinduced plasmid DNA cleavage by novel synthetic chalcones. J Photochem Photobiol B 102:200–208
11. Khan SA, Razvi MAN, Bakry AH, Afzal SM, Asiri AM, El-Daly SA (2015) Photogeneration of reactive oxygen species and photoinduced plasmid DNA cleavage by novel synthetic chalcones. Spectrochim Acta Part A 137:1100–1105
12. Schraub M, Kim H, Hampp N (2014) Photoinduced refractive index changes of 3-phenyl-coumarin containing polymers for ophthalmic applications. Eur. Polym J 51:21–27
13. Fayed TA, Awad MK (2004) Dual emission of chalcone-analogue dyes emitting in the red region. Chem Phys 303:317–326
14. Devi JM, Tharmaraj P, Ramakrishnan SK, Ramachandran K (2008) On the thermal properties of metal (II) complexes of chalcone. Mater Lett 62:852–856
15. Gaber M, El-Daly SA, Fayed TA, El-Sayed YS (2008) Photophysical properties, laser activity and photoreactivity of a heteroaryl chalcone: a model of solvatochromic fluorophore. Opt Laser Technol 40:528–537
16. El-Daly SA, Asiri AM, Khan SA, Alamry KA (2013) Spectral Properties and Micellization of 1-(2, 5-Dimethyl-thiophen-3-yl)-3-(2, 4, 5-trimethoxy-phenyl)-propenone (DTTP) in different media. J Lumin 134:819–824
17. Agilent CrysAlis PRO (2012). Agilent Technologies, Yarnton, England
18. Sheldrick GM (2008) A short history of *SHELX*. Acta Crystallogr A64:112–122
19. Barbour LJ, Seed X (2001) A software tool for supramolecular crystallography. J Supramol Chem 1:189
20. Macrae CF, Edgington PR, McCabe P, Pidcock E, Shields GP, Taylor R, Towler M, Streek JV (2006) Mercury: visualization and analysis of crystal structures. J Appl Crystallogr 39:453–457
21. Farrugia LJ (2012) *WinGX* and *ORTEP for Windows*: an update. J Appl Crystallogr 45(2012):849–854
22. Spek AL (2009) Structure validation in chemical crystallography. Acta Crystallogr D65:148–155
23. Dolomanov OV, Bourhis LJ, Gildea RJ, Howard JAK, Puschmann H (2009) *OLEX2*: a complete structure solution, refinement and analysis program. J Appl Crystallogr 42:339–341
24. Asiri AM, Akkurt M, Khan SA, Arshad MN, Khan IU, Sharif HMA (2009) 2-Benzenesulfonamidobenzoic acid. Acta Crystallogr E65: 1246–1247
25. Asiri AM, Marwani HM, Alamry KA, Al-Amoudi MS, Khan SA, El-Daly SA (2014) Green synthesis, characterization, photophysical and electrochemical properties of bis-chalcones. Int J Electrochem Sci 9: 799–809
26. Lippert E (1957) Spectroscopic determinations of the dipole moment of aromatic compounds in the first excited singlet state. Z Elektrochem 61:962–975
27. Dey JK, Dogra SK (1991) Solvatochromism and Prototropism in 2-(Aminophenyl) Benzothiazoles. Bull Chem Soc Jpn 64:3142–3152
28. Acree WE, Wilkins DC, Tucker SA, Griffin JM, Powell JR (1994) Spectrochemical investigations of preferential solvation. 2. compatibility of thermodynamic models versus spectrofluorometric probe methods for tautomeric solutes dissolved in binary mixtures, excited-state dipole moments of some hydroxycoumarin dyes using an efficient solvatochromic method based on the solvent polarity parameter, E_T^N. J Phys Chem 98:2537–2544
29. Kumar S, Rao VC, Rastogi RC (2001) Excited state dipole moments from an efficient analysis of solvatochromic stokes shift data. Spectrochim Acta A 57:41–47
30. Ravi M, Samanta A, Radhakrishnan TP (1994) Excited state dipole moments from an efficient analysis of solvatochromic stokes shift data. J Phys Chem 98:9133–9136
31. Ravi M, Soujanya T, Samanta A, Radhakrishnan TP (1995) Excited-state dipole moments of some coumarin dyes from a solvatochromic method using the solvent polarity parameter, E^N_T. J Chem Soc Faraday Trans 91:2739–2742
32. Turro NJ (1995) Molecular photochemistry (frontiers in chemestry), 1st edn. W. A. Benjamin, Inc, Reading, p 286
33. Coe BJ, Harris JA, Asselberghs I, Clays K, Olbrechts G, Persoons A, Hupp JT, Johnson RC, Coles SJ, Hursthouse MB, Nakatani K (2002) Quadratic nonlinear optical properties of N-aryl stilbazolium dyes. Adv Funct Mater 12:110–116
34. Khan SA, Asiri AM (2013) Synthesis of novel pyrazole containing Schiff base derivatives as antibacterial agents on the bases of in-vitro and DFT. Eur J Chem 4:454–458